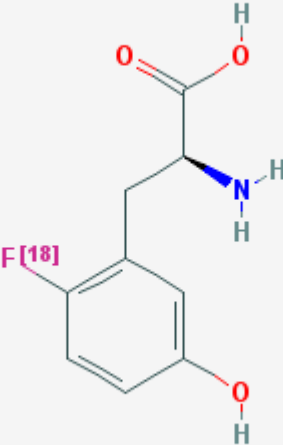


6-[¹⁸F]Fluoro-L-*m*-tyrosine

6-[¹⁸F]FMT

The MICAD Research Team

Created: May 22, 2006; Updated: September 6, 2006.

| | | |
|-----------------------------|---|--|
| Chemical name: | 6-[¹⁸ F]Fluoro-L- <i>m</i> -tyrosine |  |
| Abbreviated name: | 6-[¹⁸ F]FMT | |
| Synonym: | [¹⁸ F]FMT | |
| Agent Category: | Compound | |
| Target: | Aromatic L-amino acid decarboxylase (AAAD) | |
| Target Category: | Enzyme-substrate | |
| Method of detection: | Positron Emission Tomography (PET) | |
| Source of signal: | ¹⁸ F | |
| Activation: | No | |
| Studies: | <ul style="list-style-type: none">• <i>In vitro</i>• Rodents• Non-human primates• Humans | |
| | | Click on the above structure for additional information in PubChem . |

Background

[[PubMed](#)]

6-[¹⁸F]Fluoro-L-*m*-tyrosine (6-[¹⁸F]FMT) is a noncatecholic radioligand developed for positron emission tomography (PET) imaging of dopaminergic metabolism and function

NLM Citation: The MICAD Research Team. 6-[¹⁸F]Fluoro-L-*m*-tyrosine. 2006 May 22 [Updated 2006 Sep 6]. In: Molecular Imaging and Contrast Agent Database (MICAD) [Internet]. Bethesda (MD): National Center for Biotechnology Information (US); 2004-2013.

in the central nervous system (CNS). It is an analog of dihydroxyphenylalanine (L-DOPA) labeled with ^{18}F , a positron emitter with a physical $t_{1/2}$ of 109.7 min.

Dopamine is an important neurotransmitter that regulates and controls human movement, motivation, and cognition (1). It is also associated with human behaviors such as reward, reinforcement, and addiction. There are four main dopaminergic pathways in the CNS (2). Two pathways originating in the ventral tegmental area project toward the cortex and the limbic area, a third pathway projects from the hypothalamus projects toward the pituitary gland, and a fourth pathway projects from the substantia nigra to the striatum. Neurons located in these pathways release dopamine as a neurotransmitter at their terminals. There are five known dopamine receptor subtypes, D₁-like or D₂-like (3). The D₁-like receptor subtypes (D₁ and D₅) coupled with the G_s protein activate adenylyl cyclase, and the D₂-like subtypes (D₂, D₃, and D₄) coupled with G proteins inhibit adenylate cyclase. Abnormal changes in the dopaminergic system can lead to pathological conditions such as Parkinson's disease (PD), schizophrenia, Huntington's disease, depression, Gilles de la Tourette syndrome, narcolepsy and other neuropsychiatric disorders (4).

Radiotracer imaging with specific radiolabeled molecular probes can measure pre-, post-, and intra-synaptic aspects of the dopaminergic system (4). [^{18}F]Fluoro-L-dopa ([^{18}F]FDOPA) was the first presynaptic probe developed by Firnau et al. (5) and the first molecular probe used by Garnett et al. (6). to visualize human brain dopamine *in vivo*. Like endogenous L-DOPA, [^{18}F]FDOPA is converted by aromatic L-amino acid decarboxylase (AAAD), an enzyme to the dopamine analog fluorodopamine. Thus, PET imaging of [^{18}F]FDOPA allows *in vivo* visualization and assessment of dopamine function in the brain. However, the use of [^{18}F]FDOPA is complicated by the peripheral metabolism of this agent. DeJesus et al. (7) proposed the synthesis and use of [^{18}F]FMT and other tyrosine analogs as possible alternative dopamine probes because they lack the enediol moiety required of catecholamine-O-methyltransferase (COMT) substrates. Three isomers of [^{18}F]FMT, 2-, 4-, and 6-[^{18}F]FMT, were initially produced and studied (8). 6-[^{18}F]FMT appeared most promising as early studies showed that it gave better image contrast and followed the dopaminergic pathway in a manner similar to that of [^{18}F]FDOPA (9, 10). However, there is evidence that 6-[^{18}F]FMT is distributed in monkey brain regions rich with AAAD-containing monoaminergic neurons which include dopaminergic, serotonergic, and noradrenergic neurons (11).

Synthesis

[PubMed]

DeJesus et al. (7, 8) reported the synthesis of 6-[^{18}F]FMT *via* direct electrophilic fluorination of D,L-*m*-tyrosine with acetyl[^{18}F]hypofluorite ([^{18}F]AcOF). [^{18}F]F₂ was produced from [^{18}O]O₂ by a two-bombardment method. The final labeled product was purified by high performance liquid chromatography (HPLC). HPLC analysis showed that approximately 80% of the D,L-*m*-tyrosine had reacted, and ^{19}F -NMR analysis

indicated that the final product was a mixture of 2-, 4-, and 6-[¹⁸F]FMT isomers in the proportion of approximately 36:11:52, respectively. The radiochemical yield was $71 \pm 5\%$ ($n = 3$; decay correction based on [¹⁸F]AcOF activity) after purification. The specific activity was 3.7-7.4 GBq/mmol (100-200 mCi)/mmol).

Namavari et al. (12) described the synthesis of 6-[¹⁸F]FMT based on a regioselective radiofluorodestannylation procedure. In this method, *N*-(trifluoroacetyl)-3-acetoxy-6-(trimethylstannyl)-*L*-phenylalanine ethyl ester was first synthesized as a precursor. The radiosynthesis was carried out by electrophilic fluorodestannylation of the precursor and followed by exhaustive deprotection of the acid, amine, and phenol. More than 99% of the 6-[¹⁸F]FMT was chemically and radiochemically pure. Chiral HPLC determined the enantiomeric purity to be >99% and the total tin determined by inductively coupled plasma spectrometry was <15 parts per billion (ppb). The total synthesis time was 60 min, and the radiochemical yield was 17% of the decay-corrected ¹⁸F activity recovered from the target.

VanBrocklin et al. (13) prepared a new di-Boc protected precursor, *N*-(*tert*-butoxycarbonyl)-3-(*tert*-butoxycarbonyloxy)-6-trimethylstannyl-*L*-phenylalanine ethyl ester for electrophilic fluorination. This precursor was synthesized from *D,L-m*-tyrosine in four steps with an overall yield of 26-27%. The enantiomeric purity was >95%. Decay-corrected radiochemical yields ($n > 6$) for a two-pot method and one-pot method were $26 \pm 3\%$ and $25 \pm 6\%$, respectively. For both methods, the chemical and radiochemical purities were >96%, and the range of specific activities of 6-[¹⁸F]FMT was 28-74 MBq/ μ mol (0.75-2 Ci/mmol). The amount of total tin was <5-40 ppb.

In Vitro Studies: Testing in Cells and Tissues

[PubMed]

DeJesus et al. (14) used rat striatal synaptosomes to determine that the K_m and V_{max} of 6-[¹⁸F]FMT were 53 μ M and 390 pmol/min/g, respectively. In contrast, *L*-DOPA had a K_m of 125 μ M and V_{max} of 98 pmol/min per g. Nahmias et al. (15) found that *in vitro* incubation of 6-[¹⁸F]FMT in human whole blood showed that it took approximately 1 h for 6-[¹⁸F]FMT to equilibrate between plasma and erythrocytes. In comparison, [¹⁸F]fluorodeoxyglucose equilibrated instantaneously.

Animal Studies

Rodents

[PubMed]

Barrio et al. (9) conducted regional brain distribution and peripheral metabolism of 6-[¹⁸F]FMT in rats. Each rat received 51.8 MBq/kg (1.4 mCi/kg) radioactivity by i.v. administration and 5 mg/kg carbidopa (AAAD inhibitor) subcutaneously 60 min before the radioligand injection. HPLC analysis of rat striatal tissue 30 min after injection

revealed that the main metabolite ($54 \pm 4\%$ of radioactivity) was 6- ^{18}F fluoro-*m*-tyramine (6- ^{18}F FMA), a product of AAAD-mediated decarboxylation. Without carbidopa pretreatment, both the cerebellum activity and total striatum activity of 6- ^{18}F FMA appeared to increase. Rahman et al. (16) reported that the AAAD activity in rat serum was 60 pmol/min per ml.

In an *in vivo* microdialysis study of striatal 6- ^{18}F FMT metabolism in conscious freely moving rats, Jordan et al. (17) injected benserazide (decarboxylation inhibitor, 50 mg/kg i.p.) 30-150 min before i.v. administration of 6- ^{18}F FMT (25 mg/kg). The study found that ^{18}F fluoro-3-hydroxyphenylacetic acid (^{18}F FPAC) was the major metabolite in the striatum at 20-120 min after injection. The concentrations of 6- ^{18}F FMT and ^{18}F FPAC were 0.2-0.3 nM (peak concentration within 20 min) and 3.2-3.3 nM (peak concentration within 40 min), respectively. ^{18}F FMA was below the limit of HPLC/electrochemical quantitation in all microdialysate samples. The authors suggested that 6- ^{18}F FMA existed briefly prior to its rapid oxidation into ^{18}F FPAC. The 6- ^{18}F FMT and ^{18}F FPAC concentration profiles were similar in control and reserpinized rats. Treatment with 2.5 mg/kg amphetamine i.p. at 120 min after 6- ^{18}F FMT injection caused a transient rise in the microdialysate ^{18}F FPAC concentration in control rats but not in reserpinized rats. The authors believed this was related to the ability of amphetamine to release presynaptic dopamine store. In addition, ^{18}F FMT and its metabolites peaked at 40 min and remained in the extracellular space at a relatively constant level for the next 40-160 min after injection suggesting trapping of ^{18}F FPAC. In contrast, ^{18}F FDOPA and its metabolites, which also peaked at 40 min, cleared the brain with a $t_{1/2}$ of about 2 h (18).

Other Non-Primate Mammals

[PubMed]

No publication is currently available.

Non-Human Primates

[PubMed]

DeJesus et al. (10) conducted a comparison study between fluorinated *m*-tyrosine analogs and ^{18}F FDOPA in monkeys. Three monkeys were pretreated with carbidopa (2 mg/kg) 1 h before receiving 159.1-214.6 MBq (4.3-5.8 mCi) of 6- ^{18}F FMT. PET imaging up to 90 min showed that ^{18}F FDOPA had higher extracerebral radioactivity localization than 6- ^{18}F FMT. The striatum/cerebellum ratios at 85 min were 5.8 and 2.8 for 6- ^{18}F FMT and ^{18}F FDOPA, respectively. The mean K_i (min^{-1}) values were 0.0187 ± 0.0005 ($n=3$) and 0.0089 ± 0.0005 ($n=5$) for 6- ^{18}F FMT and ^{18}F FDOPA, respectively. HPLC analysis of blood metabolites showed that 6- ^{18}F FMT had two metabolites, and one was identified as 6- ^{18}F FPAC.

Jordan et al. (19) studied the kinetics and metabolism of 6- ^{18}F FMT in monkeys rendered hemi-Parkinsonian by unilateral intracarotid artery infusion of the neurotoxin

1-methyl-4-phenyl-1,2,3,6-tetrahydropyridine (MPTP). Four monkeys received 99.9 MBq/kg (2.7 mCi/kg) of 6-[¹⁸F]FMT (specific activity = 18.5 GBq/mM(0.5 Ci/mM) by i.v. administration. HPLC analysis of postmortem brain sections indicated that [¹⁸F]FPAC was the predominant metabolite with highest concentrations in dopaminergic regions at 60 and 120 min after injection. The 6-[¹⁸F]FMT metabolism profile was similar in treated and untreated animals. Other PET imaging studies used this MPTP monkey model to show that striatal 6-[¹⁸F]FMT uptake was altered in MPTP-treated animals (20-23). Both 6-[¹⁸F]FMT and [¹⁸F]FDOPA K_i values clearly differentiated MPTP-lesioned animals from normal animals (20). However, it was not possible to use 6-[¹⁸F]FMT k_{loss} (loss of radioactivity out of the striatum) or k_{loss}/K_i (a measure of dopamine turnover) values to differentiate MPTP-lesioned animals from normal animals whereas it was possible with the [¹⁸F]FDOPA k_{loss} or k_{loss}/K_i values. Another study comparing 6-[¹⁸F]FMT and [¹⁸F]FDOPA in aging monkeys suggested that 6-[¹⁸F]FMT might be more suitable for assessing CNS AAD activity and that [¹⁸F]FDOPA might be better in tracing dopamine turnover (24). Eberling et al (25). proposed that 6-[¹⁸F]FMT PET imaging could be used to monitor AAD gene expression by a simple ratio method.

In a study of 3 monkeys, Brown et al. (11) found that 6-[¹⁸F]FMT radioactivity localization did not correlate with dopamine concentration in other brain regions. On the other hand, localization of 6-[¹⁸F]FMT radioactivity appeared to significantly correlate with regional AAD activity ($r = 0.97$). DeJesus et al. (24) used 6-[¹⁸F]FMT (118-222 MBq/dose (3.2-6 mCi/dose) PET imaging to study aging monkey brains. Insignificant correlation was found between 6-[¹⁸F]FMT radioactivity in young (3-11 years, $n = 8$) and older (25-37 years, $n = 6$) animals. The authors suggested that AAD activity was maintained or increased in the aging monkey striatum. This result was confirmed by Eberling et al. (26). DeJesus et al (27). also reported that the *in vivo* turnover $t_{1/2}$ of the enzyme AAD in the striatum of normal monkeys after irreversible inhibition to be 86 h.

Human Studies

[PubMed]

Firnau et al. (28) studied the brain accumulation of 6-[¹⁸F]FMT and its synthesized metabolite, [¹⁸F]FPAC, up to 2 h in a healthy volunteer. The i.v. doses of both radiolabeled compounds were 111 MBq (3 mCi). The study reported that exogenously administered [¹⁸F]FPAC radioactivity in the brain was only about 5% of that of 6-[¹⁸F]FMT. In comparison, exogenous *O*-methylated (OMe[¹⁸F]DOPA) radioactivity accumulated to about ½ that of [¹⁸F]FDOPA radioactivity in all regions of the brain.

Nahmias et al. (29) performed 6-[¹⁸F]FMT PET imaging in 6 normal volunteers and 1 patient with PD. Each subject received 185-370 MBq (5-10 mCi; specific activity = 74 GBq/mM(2 Ci/mM) radioactivity and was not pretreated with carbidopa. In the normal volunteers, radioactivity accumulated in the dopamine-rich areas, the caudate nucleus and the putamen. In the PD patient, little radioactivity accumulation was observed in the putamen contralateral to the side exhibiting clinical symptoms. The mean striatum/

cerebellum ratio was 4.95 ± 1.16 ($n = 6$), and the mean influx rate K_c for the striatum was 0.0171 ± 0.0018 ml/min per g. In comparison, [^{18}F]FDOPA had a striatum/cerebellum ratio of 2.18 ± 0.22 ($n = 19$). Blood samples analyzed by chromatography indicated that the percentages of intact 6-[^{18}F]FMT were 69% at 10 min and 49% at 90 min. In one volunteer who did a repeated study and was pretreated with 5 mg/kg carbidopa, the percentages of intact 6-[^{18}F]FMT were 91% at 10 min and 70% at 90 min. The study also indicated that data from the striatal, cortical, and cerebellar time-activity curves were best fitted by a two-compartment, three-parameter model. Asselin et al. (30) in a study of blood data collected on 30 human subjects injected with 6-[^{18}F]FMT proposed that a three-compartment four-parameter model gave significantly better fits to the blood data.

Asselin et al. (31) described striatal patterns of 6-[^{18}F]FMT distribution in 21 patients for differential diagnoses of PD and other movement disorders. It was reported that the striatal 6-[^{18}F]FMT distribution pattern can be used to classify patients by the following diagnoses: (a) normal, essential tremor and DOPA-responsive dystonia, (b) progressive supranuclear palsy and multiple system atrophy (MSA), (c) unilateral PD, (d) bilateral PD, MSA, and late-onset dystonia, and (e) corticobasal degeneration.

References

1. Volkow ND, Fowler JS, Gatley SJ, Logan J, Wang GJ, Ding YS, Dewey S. PET evaluation of the dopamine system of the human brain. *J Nucl Med.* 1996;37(7): 1242–1256. PubMed PMID: 8965206.
2. Dailly E, Chenu F, Renard CE, Bourin M. Dopamine, depression and antidepressants. *Fundam Clin Pharmacol.* 2004;18(6):601–607. PubMed PMID: 15548230.
3. 3. Wagner HN, Szabo Z. Research and clinical applications of neuroreceptor imaging, in *Handbook of Radiopharmaceuticals*, M.J. Welch and C.S. Redvanly, Editors. 2003, John Wiley & Sons, Ltd: West Sussex, England. p. 582-602.
4. Verhoeff NP. Radiotracer imaging of dopaminergic transmission in neuropsychiatric disorders. *Psychopharmacology (Berl).* 1999;147(3):217–249. PubMed PMID: 10639681.
5. Firna G, Nahmias C, Garnett S. The preparation of (^{18}F)5-fluoro-DOPA with reactor-produced fluorine-18. *Int J Appl Radiat Isot.* 1973;24(3):182–184. PubMed PMID: 4689915.
6. Garnett ES, Firna G, Nahmias C. Dopamine visualized in the basal ganglia of living man. *Nature.* 1983;305(5930):137–138. PubMed PMID: 6604227.
7. DeJesus OT, Mukherjee J, Appelman EH. Synthesis of O- and M-tyrosine analogs as potential tracers for CNS dopamine. *J. Label. Comp. Radiopharm.* 1989;26:133–134.
8. DeJesus OT, Sunderland JJ, Nickles JR, Mukherjee J, Appelman EH. Synthesis of radiofluorinated analogs of m-tyrosine as potential L-dopa tracers via direct reaction with acetylhypofluorite. *Int J Rad Appl Instrum [A].* 1990;41(5):433–437. PubMed PMID: 2166010.
9. Barrio JR, Huang SC, Yu DC, Melega WP, Quintana J, Cherry SR, Jacobson A, Namavari M, Satyamurthy N, Phelps ME. Radiofluorinated L-m-tyrosines: new in-

- vivo probes for central dopamine biochemistry. *J Cereb Blood Flow Metab.* 1996;16(4):667–678. PubMed PMID: 8964807.
10. DeJesus OT, Endres CJ, Shelton SE, Nickles RJ, Holden JE. Evaluation of fluorinated m-tyrosine analogs as PET imaging agents of dopamine nerve terminals: comparison with 6-fluoroDOPA. *J Nucl Med.* 1997;38(4):630–636. PubMed PMID: 9098215.
 11. Brown WD, DeJesus OT, Pyzalski RW, Malischke L, Roberts AD, Shelton SE, Uno H, Houser WD, Nickles RJ, Holden JE. Localization of trapping of 6-[(¹⁸F)]fluoro-L-m-tyrosine, an aromatic L-amino acid decarboxylase tracer for PET. *Synapse.* 1999;34(2):111–123. PubMed PMID: 10502310.
 12. Namavari M, Satyamurthy N, Phelps ME, Barrio JR. Synthesis of 6-[¹⁸F] and 4-[¹⁸F]fluoro-L-m-tyrosines via regioselective radiofluorodestannylation. *Appl Radiat Isot.* 1993;44(3):527–536. PubMed PMID: 8472025.
 13. VanBrocklin HF, Blagoev M, Hoeppling A, O'Neil JP, Klose M, Schubiger PA, Ametamey S. A new precursor for the preparation of 6-[¹⁸F]Fluoro-L-m-tyrosine ([¹⁸F]FMT): efficient synthesis and comparison of radiolabeling. *Appl Radiat Isot.* 2004;61(6):1289–1294. PubMed PMID: 15388123.
 14. DeJesus OT, Murali D, Nickles RJ. *Synthesis of brominated and fluorinated ortho-tyrosine analogs as potential DOPA decarboxylase tracers.* *J Label. Comp. Radiopharm.* 1995;37:147–149.
 15. Nahmias C, Wahl LM, Amano S, Asselin MC, Chirakal R. Equilibration of 6-[¹⁸F]fluoro-L-m-tyrosine between plasma and erythrocytes. *J Nucl Med.* 2000;41(10):1636–1641. PubMed PMID: 11037992.
 16. Rahman MK, Nagatsu T, Kato T. Determination of aromatic L-amino acid decarboxylase in serum of various animals by high-performance liquid chromatography with electrochemical detection. *Life Sci.* 1981;28(5):485–492. PubMed PMID: 6970873.
 17. Jordan S, Bankiewicz KS, Eberling JL, VanBrocklin HF, O'Neil JP, Jagust WJ. An in vivo microdialysis study of striatal 6-[¹⁸F]fluoro-L-m-tyrosine metabolism. *Neurochem Res.* 1998;23(4):513–517. PubMed PMID: 9566585.
 18. DeJesus OT, Haaparanta M, Solin O, Nickles RJ. 6-fluoroDOPA metabolism in rat striatum: time course of extracellular metabolites. *Brain Res.* 2000;877(1):31–36. PubMed PMID: 10980240.
 19. Jordan S, Eberling JL, Bankiewicz KS, Rosenberg D, Coxson PG, VanBrocklin HF, O'Neil JP, Emborg ME, Jagust WJ. 6-[¹⁸F]fluoro-L-m-tyrosine: metabolism, positron emission tomography kinetics, and 1-methyl-4-phenyl-1,2,3,6-tetrahydropyridine lesions in primates. *Brain Res.* 1997;750(1-2):264–276. PubMed PMID: 9098552.
 20. Doudet DJ, Chan GL, Jivan S, DeJesus OT, McGeer EG, English C, Ruth TJ, Holden JE. Evaluation of dopaminergic presynaptic integrity: 6-[¹⁸F]fluoro-L-dopa versus 6-[¹⁸F]fluoro-L-m-tyrosine. *J Cereb Blood Flow Metab.* 1999;19(3):278–287. PubMed PMID: 10078880.
 21. Eberling JL, Jagust WJ, Taylor S, Bringas J, Pivrotto P, VanBrocklin HF, Bankiewicz KS. A novel MPTP primate model of Parkinson's disease: neurochemical and clinical changes. *Brain Res.* 1998;805(1-2):259–262. PubMed PMID: 9733979.

22. Eberling JL, Pivrotto P, Bringas J, Bankiewicz KS. Tremor is associated with PET measures of nigrostriatal dopamine function in MPTP-lesioned monkeys. *Exp Neurol*. 2000;165(2):342–346. PubMed PMID: 10993693.
23. Eberling JL, Pivrotto P, Bringas J, Bankiewicz KS. Comparison of two methods for the analysis of [18F]6-fluoro-L-m-tyrosine PET data. *Neuroimage*. 2004;23(1):358–363. PubMed PMID: 15325383.
24. Dejesus OT, Endres CJ, Shelton SE, Nickles RJ, Holden JE. Noninvasive assessment of aromatic L-amino acid decarboxylase activity in aging rhesus monkey brain in vivo. *Synapse*. 2001;39(1):58–63. PubMed PMID: 11071710.
25. Eberling JL, Cunningham J, Pivrotto P, Bringas J, Daadi MM, Bankiewicz KS. In vivo PET imaging of gene expression in Parkinsonian monkeys. *Mol Ther*. 2003;8(6):873–875. PubMed PMID: 14664788.
26. Eberling JL, Roberts JA, Taylor SE, VanBrocklin HF, O'Neil JP, Nordahl TE. No effect of age and estrogen on aromatic L- amino acid decarboxylase activity in rhesus monkey brain. *Neurobiol Aging*. 2002;23(3):479–483. PubMed PMID: 11959410.
27. DeJesus OT, Flores LG, Murali D, Converse AK, Bartlett RM, Barnhart TE, Oakes TR, Nickles RJ. Aromatic L-amino acid decarboxylase turnover in vivo in rhesus macaque striatum: a microPET study. *Brain Res*. 2005;1054(1):55–60. PubMed PMID: 16055094.
28. Firnau G, Chirakal R, Nahmias C, Garnett ES. Do the metabolites of [18F]Fluoro-L-Dopa and [18F]Fluoro-meta-Tyrosine contribute to the accumulation of [18F] in the human brain? *Label. Comp. Radiopharm*. 1991;30:293–294.
29. Nahmias C, Wahl L, Chirakal R, Firnau G, Garnett ES. A probe for intracerebral aromatic amino-acid decarboxylase activity: distribution and kinetics of [18F]6-fluoro-L-m-tyrosine in the human brain. *Mov Disord*. 1995;10(3):298–304. PubMed PMID: 7651447.
30. Asselin MC, Wahl LM, Cunningham VJ, Amano S, Nahmias C. In vivo metabolism and partitioning of 6-[18F]fluoro-L-meta-tyrosine in whole blood: a unified compartment model. *Phys Med Biol*. 2002;47(11):1961–1977. PubMed PMID: 12108778.
31. Asselin MC, Amano S, Chirakal R, Thompson M, Nahmias C. Patterns of distribution of [18F]6fluoro-L-m-tyrosine in PET images of patients with movement disorders, in *Brain Imaging Using PET*, M. Senda, Y. Kimura, and P. Herscovitch, Editors. 2002, New York Academic Press: New York.